CHAPTER 4

OPERATION PRINCIPLES OF TUNABLE EXTERNAL-CAVITY DIODE LASERS

In this chapter first we introduce the basic principles of the grating-tuned external-cavity diode lasers (ECDL) in Sec. 4.1, and then follow up with a brief introduction of the nematic liquid crystals (NLC) in Sec. 4.2. In Sec 4.3 and Sec. 4.4, two types of NLC elements, a planar-aligned NLC cell and a liquid crystal pixel mirror (LCPM), used in the ECDL systems are introduced.

4.1 Tunable ECDL

A tunable ECDL comprises a semiconductor gain chip with antireflection (AR) coating on one facet, optics for coupling the output of the gain-media waveguide to the free space mode of the external cavity, one or more wavelength selective filters, and a retroreflecting end mirror for defining the external feedback path. Diffraction gratings in ECDL's combine the functions of the filter and external mirror. Two common retro-reflecting mounting geometries for diffraction gratings in ECDL's are the Littrow (Fig. 4.1) and the grazing-incidence (Littman-Metcalf, Fig. 4.2) configurations.

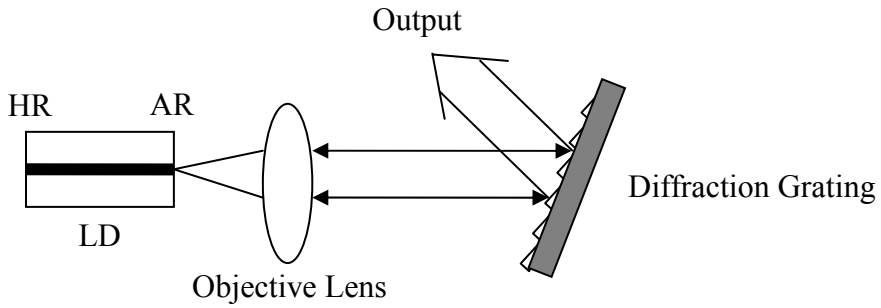

Fig. 4.1 ECDL in the Littrow configuration. LD: laser diode; HR: high reflector; AR: anti-reflection coating

In the Littrow configuration, the angles of incident and diffraction are equal. In the Littman configuration, the intracavity beam makes two passes at the grating. The two end mirrors of

the laser cavity are the facet of LD, which is coated as a high reflector (HR) and the grating in the Littrow configuration or the feedback mirror in the Littman configuration. In any external-cavity design, one should try to maximize the external feedback strength and wavelength selectivity of the cavity. The Littman-Metcalf cavity employs a double pass grazing incidence cavity that naturally achieves multi-mode suppression. The mirror angle becomes the tuning mechanism.

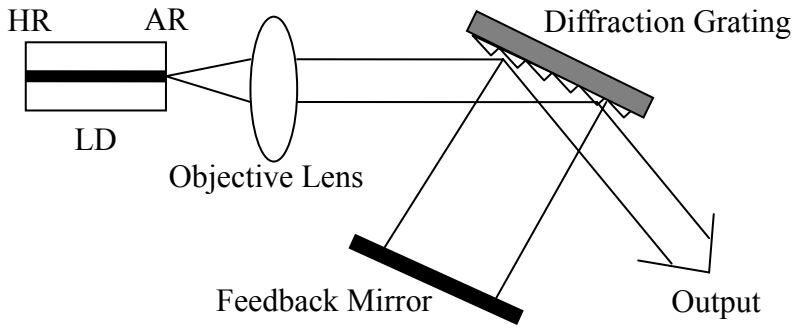

Fig. 4.2 ECDL in the grazing-incidence configuration

4.1.1 Diffraction gratings [66]

Diffraction gratings are the most common type of filter used in ECDL's. When a beam of light is incident on a grating, each groove generates a diffracted wavelet. For each wavelength component in the incident beam, the constructive interference of the diffracted components from each groove occurs at a unique set of discrete directions called diffraction orders of the grating. The familiar grating equation is expressed as

$$a(\sin\theta_i + \sin\theta_m) = m\lambda \tag{4.1}$$

where a is the groove spacing, θ_i is the incident angle, θ_m is the angle of the m^{th} order diffraction, and m is the diffraction order. The light is dispersed with different wavelengths at different angles of diffraction. The wavelength resolution of a grating-tuned external cavity is determined by the angular dispersion multiplied by the acceptance angle for coupling back into the active region of the gain medium. The angular dispersion can therefore be used as a figure of merit, but it must be remembered that the parameter of ultimate importance is the grating resolution divided by the axial mode spacing of the external cavity. Diffraction gratings in external-cavity lasers combine the functions of the filter and external mirror. In

extended cavity, the light from the grating must be retro-reflected back into the gain medium. In the Littrow configuration, the angles of incidence and diffraction are equal. The grating equation (4.1) then becomes

$$\lambda = 2a \sin\theta_i \tag{4.2}$$

In this case the angular dispersion of the retro-reflected beam is identical to that of the diffracted beam and is given by

$$D_{Littrow} = \frac{d\theta_1}{d\lambda} = \frac{2\tan\theta_i}{\lambda} \tag{4.3}$$

In the grazing-incidence configuration (Fig. 4.2), the intracavity beam makes two passes at the grating. The diffracted light from the second pass is a retro-reflection of the incident light from the first pass. Therefore, the angular dispersion of the retro-reflection light is twice that of the light diffracted on once pass

$$D_{Littman} = 2\frac{d\theta_1}{d\lambda} = \frac{4\tan\theta_i}{\lambda} = 2D_{Litrow} \tag{4.4}$$

The dispersion of the grazing-incidence configuration is therefore twice that of the Littrow configuration for the same angle of incidence. In addition, the grazing-incidence configuration is typically used with a much higher angle of incidence. To obtain greater angular dispersion it is necessary to use larger blaze and diffraction angles. This is the regime in which polarization effects become significant. For blaze angles θ_B above ~10°, the diffraction efficiency strongly depends on the orientation of optical polarization with respect to the direction of the grooves. A particularly useful regime for tuning ECDL's is the range of blaze angles from about 22°, to 38°. For this regime, there is a broad plateau of high efficiency for $\theta_i > \theta_B$ when the incident polarization is perpendicular to the direction of the grooves on the grating.

The wavelength resolution is obtained by dividing the angular spread of the beam waist at the grating (waist divergence) by the angular dispersion. The waist divergence for a Gaussian beam of radius ω_g is given by

$$\Delta\theta_{div} = \frac{\lambda}{\pi\omega_g} \tag{4.5}$$

The wavelength resolutions for the Littrow and grazing-incidence cases are, respectively

$$\Delta\lambda_{FWHM\,(Littrow)} = \frac{\Delta\theta_{div}}{D_{Littrow}} = \frac{\lambda^2}{2\pi\omega_g\theta_i} \tag{4.6}$$

$$\Delta\lambda_{FWHM\,(Littman)} = \frac{\theta_{div}}{D_{Littman}} = \frac{\lambda^2}{4\pi\omega_g\theta_i} \tag{4.7}$$

The frequency bandwidth can be expressed as

$$\Delta\nu = c\Delta\lambda/\lambda^2 \tag{4.8}$$

As an example, if the beam radius ω_g=1 mm, λ=780 nm, a = (1800 lines/mm)$^{-1}$, $\theta_{i\ (Littrow)}$ = 50°, $\theta_{i\ (Littman)}$ = 80°, we obtain grating bandwidths of $\Delta\lambda_{\ (Littrow)}$ = 0.11 nm, $\Delta\nu_{\ (Littrow)}$ = 54.2 GHz, $\Delta\lambda_{\ (Littman)}$ = 0.035 nm, and $\Delta\nu_{\ (Littman)}$ = 17.1 GHz. The design of grazing-incidence configuration takes the advantage of higher wavelength resolution.

4.1.2 Mode hopping

A diode laser's output spectrum depends strongly on case temperature and injection current. For example, a typical plot of wavelength versus temperature (Fig. 4.3) for a LD reveals a stair-step pattern. The wavelength shifts slowly with temperature in some regions. However, at some values of case temperature, the wavelength may make discrete jumps. These large shifts happen when the laser switches from one longitudinal mode to another, called mode hopping.

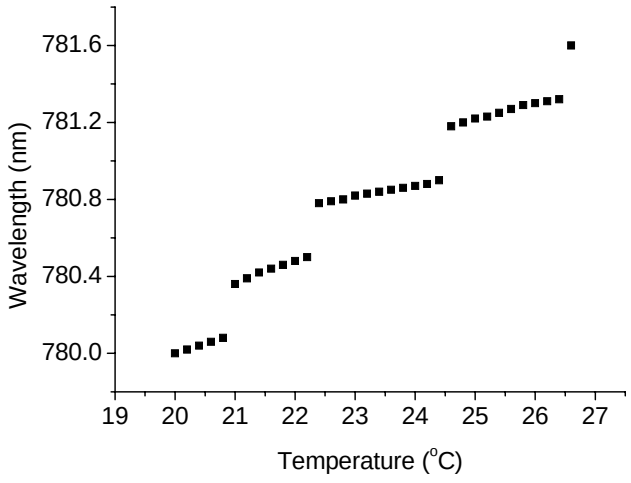

Fig. 4.3 Temperature dependence of LD wavelength

Consider an ECDL, the gain bandwidth of the diode laser is typically over 20 nm and can be as high as 100 nm, depending on wavelength and diode material. The modes of the external cavity are evenly spaced, e.g. 1 GHz for a 15-cm cavity. The intrinsic gain profile of LD media and cavity modes are plot in Fig. 4.4. Suppression of multimode behavior requires the dispersion of the cavity to have a bandwidth on this order. Since the extended-cavity length is large and the cavity mode spacing is small, there is always a finite probability that the laser will jump from one mode to the other.

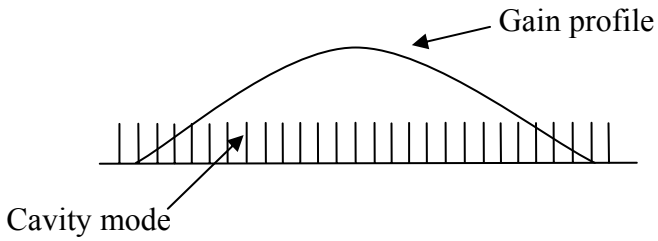

Fig. 4.4 Gain profile of LD and longitudinal cavity modes

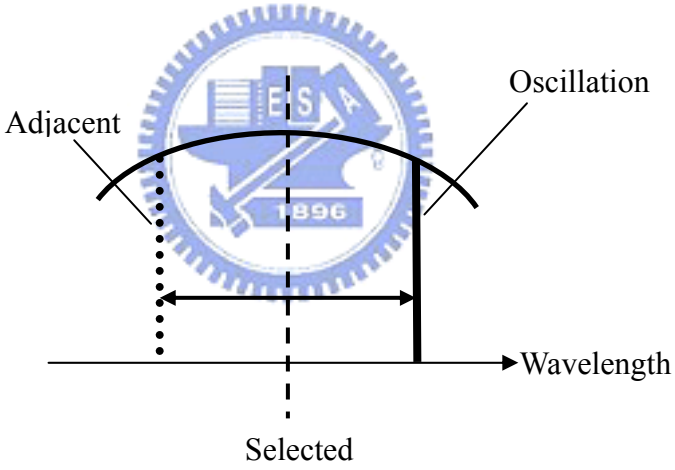

Fig. 4.5 Illustration of the cause of mode hopping

Fig. 4.5 shows a schematic diagram of the mode hopping mechanism. We define the center wavelength of the bandwidth selected by the diffraction grating as the ′selected wavelength′. The top curve shows the wavelength selectivity of the diffraction grating and the center dashed line is the selected wavelength. The right solid line is the oscillating mode and the left dotted line is the adjacent mode. Mode hopping occurs easily when the two differences in wavelength between the oscillating wavelength and selected wavelength, and between the adjacent mode and the selected wavelength, are nearly equal. When the cavity is tuned by rotating the feedback mirror in Littman-Metcalf configuration, the comb of external-cavity modes shifts proportional to the cavity length, and the selected wavelength is changed too.

Therefore, the mismatch between the change ratios of the oscillation wavelength and selected wavelength sometimes causes mode hopping. The mode closet to the selected wavelength oscillates, so mode hopping occurs cyclically at wavelength sweeping [67-69]. Mode hopping is undesirable in many applications. In telecommunications, for example, the switching from one mode to another affects the maximum data transmission rate, because different velocities in single mode fibers with high dispersion. Spectroscopy is another area that usually requires wavelength can be continuously swept over certain range.

4.2 Nematic liquid crystals

There are several distinct kinds of liquid crystalline phases reported. In general, liquid crystal can be divided into three different phases, smectics, nematics and cholesterics. The common characteristic of these phases is that they are stable in a temperature range, which is between the temperature ranges where the isotropic liquid and the solid phase are stable. For this reason they also referred to as mesophases, meaning middle phases. In this thesis, we only concern with the nematic phase. It was Friedel who first gave the name nematic from the Greek word *nema*, meaning thread, because of the thread-like discontinuities which can be observed under the polarizing microscope for this phase. The nematic phase has the lowest ordering of all the mesophases. The centres of gravity of the molecules have no long-range order. The molecules making up the nematic phase are arranged in such a manner that there is no positional order of their centers of mass, like ordinary liquid. There is some order, however, in the direction of the molecules. They tend to orient on the average along a preferred direction within a large cluster of molecules, called the director **n**. Optically, a nematic is a uniaxial medium with the optical axis along **n**. The states of director **n** and –**n** are indistinguishable [70]. The molecular orientation can be controlled with applied electric or magnetic fields. Within a sufficiently large electric or magnetic fields, the local directors will be either parallel or perpendicular to the applied field.

Two kinds of nematic liquid crystal (NLC), 5CB and E7, were chosen for our experiments because the physical properties are well known and they are commercially available. The liquid crystal 5CB (4'-n-pentyl-4-cyanobiphenyl, Merck) has simple phase transitions. It changes from a solid to a NLC at 22.5 °C, and melts to an isotropic liquid at 35 °C. The liquid crystal E7 (Merck) is a nematic mixture. It changes from a solid to a NLC at -10 °C, and melts to an isotropic liquid at 60.5 °C. Both 5CB and E7 can be used at room temperature.

4.3 Planar-aligned NLC cell

4.3.1 Structures and basic principles

The planar-aligned NLC cell as shown in Fig. 4.6 is constructed by sandwiching a layer of NLC between two indium-tin–oxide (ITO) glass plates. The cell gap is determined by the thickness of the spacer. After assembly, the two glass plates are parallel within half a wavelength in the visible (i.e., less than 300 nm), as determined by an interference experiment. 5CB was chosen as the LC material. Planar alignment of the nematic phase is achieved by rubbing polyimide films coated on the inner sides of substrates.

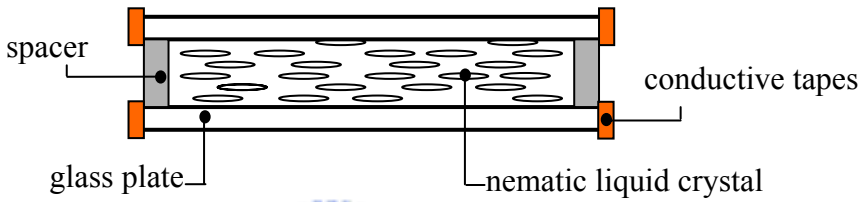

Fig. 4.6 The structure of the planar-aligned NLC cell

When NLC makes contact with a bounding surface, e.g. glass surfaces, molecules align in a certain direction called easy axis. In the planar-aligned cell, molecules are aligned parallel to the glass wall as shown in Fig. 4.7(a). If the NLC cell is now under an external magnetic or electric field, alignment of the molecules is subjected to competing effect of the field and the wall. With the increasing of the electric field the molecules at the boundary are aligned parallel to the glass wall. Molecules from the wall, however, tend to become parallel to the electric field as shown in the Fig. 4.7(b). Molecules make a uniform twist from the wall to where molecules are parallel to the field. For a sufficiently intense electric field all the molecules are aligned parallel to the electric field, which is perpendicular to the easy direction i.e. perpendicular to the surfaces of the glass substrates (Fig. 4.7(c)). Refractive indices and birefringence of the LC are practically important parameters. A uniformly aligned slab of LC material can be considered to be a uniaxial slab, having its optic axis directed along the long axis of the LC molecules. When an electric field is applied in a lateral direction across the glass plates as shown in the Fig. 4.7(b) and (c), this changes the angle between the optic axis and the incident beam direction.

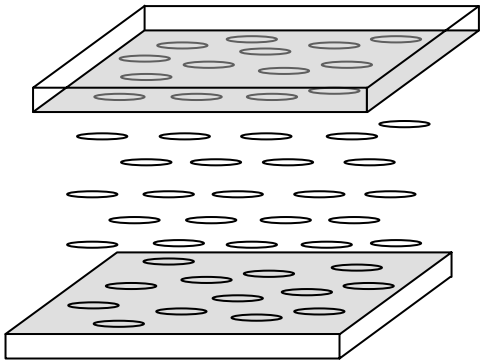

(a)

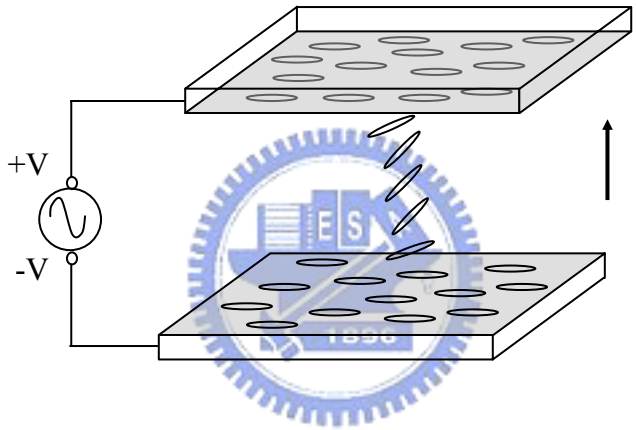

(b)

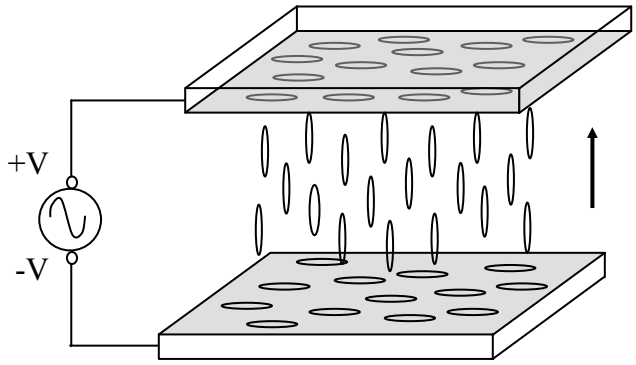

(c)

Fig. 4.7 The planar NLC cell without (a), and with (b) (c) an external electric field

In a uniaxially birefringent LC material, the refractive index of the ordinary mode is independent of the direction of light propagation, whereas the refractive index for the extraordinary mode depends on the direction of propagation. The extraordinary refractive index dependence on the angle θ between the optic axis and the incident beam direction is given by

$$n_{eff}(\theta)=\left[\frac{\sin^2(\theta)}{n_e}+\frac{\cos^2(\theta)}{n_o}\right]^{-1/2} \tag{4.9}$$

Where n_o is the ordinary refractive index and n_e is the extraordinary refractive index for θ = 90°. Thus the LC can be used as a phase retarder (Fig. 4.8).

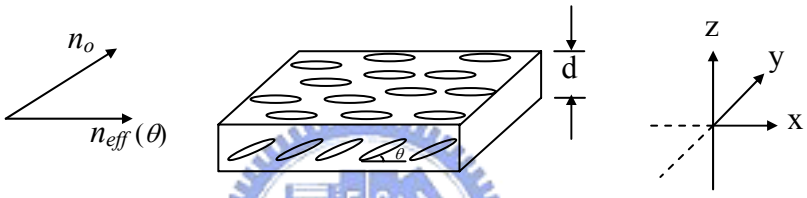

Fig. 4.8 The LC is used as a phase retarder

In general, if $\theta=\theta(z)$ then $n_{eff}(\theta)=n_{eff}(z)$, the phase retardation $\Delta\Phi$ is expressed as

$$\Delta\Phi = k\int_0^d\left[n_{eff}(z)-n_0\right]dz \tag{4.10}$$

where $k=2\pi/\lambda$, λ is the wavelength of the incident light, d is the thickness of the LC plate. The maximum phase retardation is given as

$$\Delta\Phi_{\max}=\frac{2\pi}{\lambda}(n_e-n_o)d \tag{4.11}$$

To consider a NLC cell sandwiched between two crossed polarizers, the arrangement is shown in Fig. 4.9. The transmission axis of the first polarizer makes an angle of φ with respect to the LC director. The transmission axis of the second polarizer is perpendicular to that of the first polarizer. The polarization direction of the incident light is parallel to the transmission axis of the first polarizer.

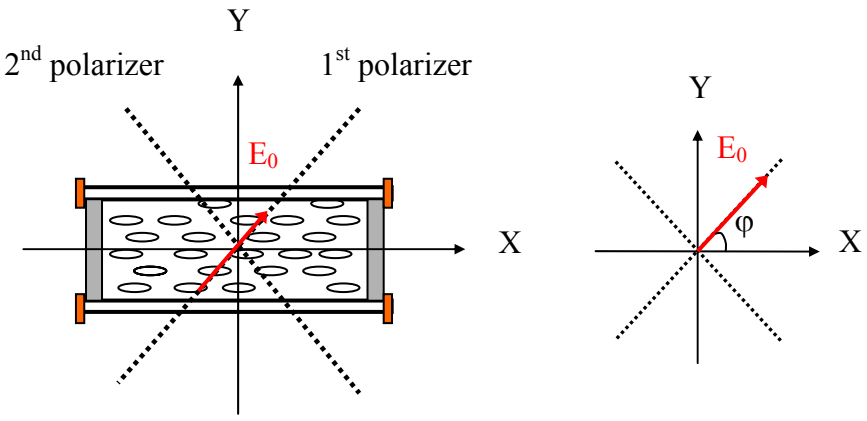

Fig. 4.9 The NLC cell sandwiched between two crossed polarizers

We describe the propagation of the incident light through the NLC cell by the Jones calculus. The Jones matrix for a phase retarder [71] is

$$\begin{bmatrix} e^{ikn_{eff}d} & 0 \\ 0 & e^{ikn_o d} \end{bmatrix} \tag{4.12}$$

A linearly polarized light passing through the NLC cell with crossed polarizers is expressed as

$$\begin{pmatrix} -\sin\varphi & \cos\varphi \end{pmatrix} \begin{pmatrix} e^{ikn_{eff}d} & 0 \\ 0 & e^{ikn_o d} \end{pmatrix} \begin{pmatrix} E_0 \cos\varphi \\ E_0 \sin\varphi \end{pmatrix} \tag{4.13}$$

The transmission intensity I of this setup can be expressed as

$$I = {E_0}^2 \sin^2 2\varphi \sin^2 \frac{\Delta\Phi}{2} = I_0 \sin^2 2\varphi \sin^2 \frac{\Delta\Phi}{2} \tag{4.14}$$

The phase retardation $\Delta\Phi$ is given by

$$\Delta\Phi = \frac{2\pi}{\lambda}(n_e - n_o)d \tag{4.15}$$

Where $(n_e - n_o)$ is the birefringence, and d is the LC thickness. The transmission maxima and minima occur when $\Delta\Phi$ is $(2N+1)\cdot\pi$ and $2N\cdot\pi$ respectively. N is an integer. If the first polarizer is oriented to be parallel to the polarization of the incident linearly polarized light, which is also at an angle of $\varphi = 45°$ to the rubbing direction of the planar NLC cell, the transmission intensity I can be derived from *Eq.* (4.14)

$$I = I_0 \sin^2 \frac{\Delta\Phi}{2} \tag{4.16}$$

4.3.2 The NLC cell in the laser cavity

We consider a planar-aligned NLC cell to be inserted in the external laser cavity. A schematic of laser configuration is shown as Fig. 4.10.

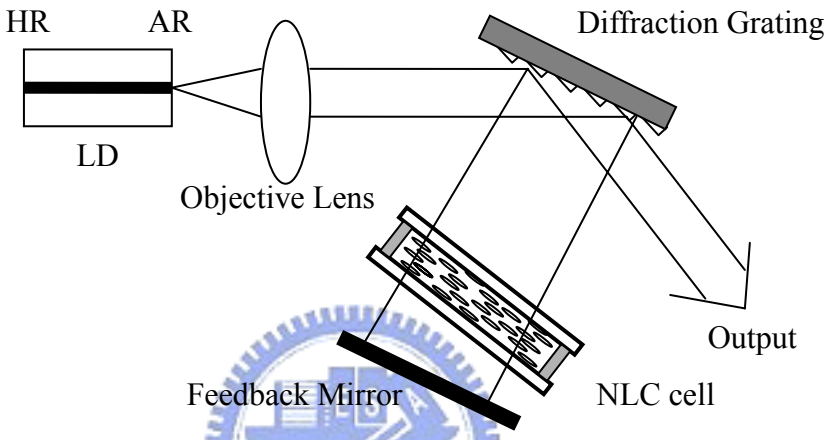

Fig. 4.10 Schematic of the ECDL with an intracavity NLC cell. HR: high reflector; AR: anti-reflection coating; NLC: nematic liquid crystal.

The NLC cell is oriented so that the laser polarization direction is along its rubbing direction. Varying the voltage driving NLC cell, its extraordinary index of refraction would change due to field-induced reorientation of the LC director and results in an additional intracavity phase retardation $\Delta\Phi$, which corresponds to an optical path difference $\Delta l = \Delta\Phi / k$. The relative frequency shift of the laser output is then given by

$$\frac{\Delta l}{l} = -\frac{\Delta f}{f} \tag{4.17}$$

where $\Delta l = \Delta n d$ is the optical path change through the NLC cell, l is the cavity length, Δf is the induced relative frequency shift, f is the laser frequency. The maximum tuning range of the LC cell is then

$$\left|(\Delta f)_{\max}\right| = f\left|n_e - n_o\right|(d/l) \tag{4.18}$$

4.3.3 Mode-hop-free tuning

For single mode oscillation and continuous wavelength tuning, the longitudinal mode spectrum of the external cavity and of the laser diode chip must be tuned synchronously [72-74]. The bias current of LD can be used as a parameter to control the longitudinal mode spectrum of the laser diode chip. The longitudinal mode spectrum of the external cavity depends on the external cavity length. Two independent cavities are involved. One is a short cavity formed by the two facets of the LD chip and has an optical length of l_1. The other is a long cavity defined by the external cavity and has an optical length of l_2. In order to scan the laser wavelength by $\Delta\lambda$ without mode hopping, the number of the longitudinal mode of each cavity must remain unchanged. The numbers of the longitudinal modes in the two cavities and the optical cavity lengths are related as following equations:

$$l_1 = N_1\lambda / 2 \tag{4.19}$$

and

$$l_2 = N_2\lambda / 2 \tag{4.20}$$

The length variations of the LD chip cavity Δl_1 and the external cavity Δl_2 necessary to achieve mode-hop-free tuning are related by

$$\Delta l_1 / l_1 = \Delta l_2 / l_2 \tag{4.21}$$

Let's define the parameter β as the ratio of wavelength change, $\Delta\lambda$, to the change of the LD drive current, ΔI_{LD}. We then obtain the relationship of ΔI_{LD} and Δl_2 by combining *Eqs*. (4.19), (4.20) and (4.21),

$$\Delta I_{LD} = \frac{\lambda \Delta l_2}{\beta\, l_2} \tag{4.22}$$

Therefore, the current of LD has to be modified when a variation of external cavity length is induced by the change of the driving voltage on NLC cell.

4.4 Liquid crystal pixel mirror

4.4.1 Structures and operation principles

The liquid crystal pixel mirror (LCPM) as shown in Fig. 4.11 is based on the design of a normally off-state twisted nematic liquid crystal (TNLC) cell bonded to a polarizer and an Au-coated silicon substrate as the back mirror. The TNLC cell is constructed with a NLC layer sandwiched between indium-tin-oxide (ITO) glass plates with the two rubbing directions are perpendicular to each other. One of the ITO electrodes is patterned.

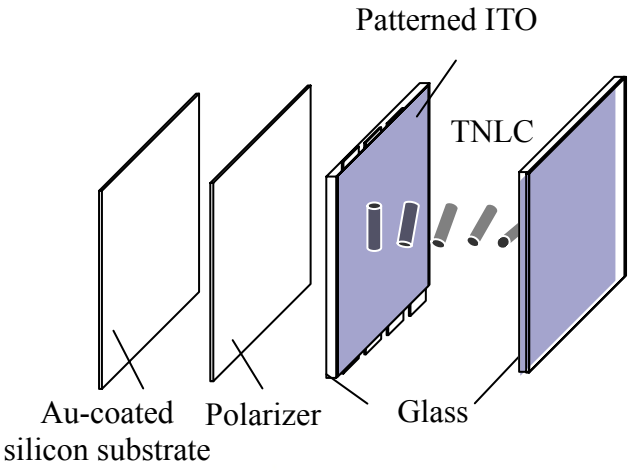

Fig. 4.11 The structure of the LCPM and ITO patterns

The LC molecules are twisted in 90° from one side to the other side of the glass. Assume the liquid crystal molecule is an ellipsoid. We can also describe the propagation of the incident light through the TNLC cell by the Jones calculus. The TNLC is not homogeneous because the direction of the director is a function of position. We divide the TNLC plate into *N* equally thin plates and assume that each plate is a wave plate with a phase retardation and an azimuth angle. We assume the twisting is linear and let Γ be the phase retardation of the plate when it is untwisted. In particular, for the case of nematic LC with c axis parallel to the plate surfaces (planar-aligned), Γ is given by

$$\Gamma = \frac{2\pi}{\lambda}(n_e - n_o)d \tag{4.23}$$

Here the phase retardation of *Eq*. (4.23) is the same as *Eq*. (4.15). We use different symbols, Γ and ΔΦ, just for easy distinguishing the TN cell from the planar cell. Thus each plate has a phase retardation of Γ/*N*, and the plates are oriented at azimuth angles ρ, 2ρ,…, *N*ρ with ρ=ϕ/*N*. ϕ is the total twist angle. The overall Jones matrix can then be obtained by multiplying together all the matrices associated with these plates.

$$M = R(\phi)\begin{pmatrix} \cos\frac{\phi}{N}e^{-i\Gamma/2N} & -\sin\frac{\phi}{N}e^{-i\Gamma/2N} \\ \sin\frac{\phi}{N}e^{i\Gamma/2N} & \cos\frac{\phi}{N}e^{i\Gamma/2N} \end{pmatrix}^N \tag{4.24}$$

where $R(\phi)$ is the rotation matrix. In the limit when $N \to \infty$, the exact expression for the Jones matrix of a linearly twisted anisotropic plate is

$$M = R(\phi)\begin{pmatrix} \cos X - i\frac{\Gamma}{2}\frac{\sin X}{X} & -\phi\frac{\sin X}{X} \\ \phi\frac{\sin X}{X} & \cos X + i\frac{\Gamma}{2}\frac{\sin X}{X} \end{pmatrix} \tag{4.25}$$

where $X = \sqrt{\phi^2 + \left(\frac{\Gamma}{2}\right)^2}$. Let P be the initial polarization state, the polarization state P′ after exiting the plate can be written as

$$P' = MP \tag{4.26}$$

Now consider the case of TNLC with a quarter turn, $\phi=(1/2)\pi$. If this layer is placed between a pair of parallel polarizers with their transmission axes parallel to the c axis of the LC at the entrance plane. The polarization state of a beam passes through the first polarizer and the LC can be written

$$P' = \begin{pmatrix} \phi\frac{\sin X}{X} \\ \cos X + i\frac{\Gamma}{2}\frac{\sin X}{X} \end{pmatrix} \tag{4.27}$$

The y component will be blocked by the second polarizer. The transmissivity of the whole structure is thus given by

$$T = \frac{\sin^2\left(\frac{1}{2}\pi\sqrt{1+\left(\Gamma/\pi\right)^2}\right)}{1+\left(\Gamma/\pi\right)^2} = \frac{\sin^2\left(\frac{\pi}{2}\sqrt{1+u^2}\right)}{1+u^2} \tag{4.28}$$

where u is the Mauguin parameter defined as $u = 2d(n_e - n_o)/\lambda$. We plot he transmission T in *Eq.*(4.28) as a function of the Mauguin parameter u. In Fig. 3.12, the values of minimum

points of u (T=0) are important parameters for designing the TNLC cell used as the spatial light modulator.

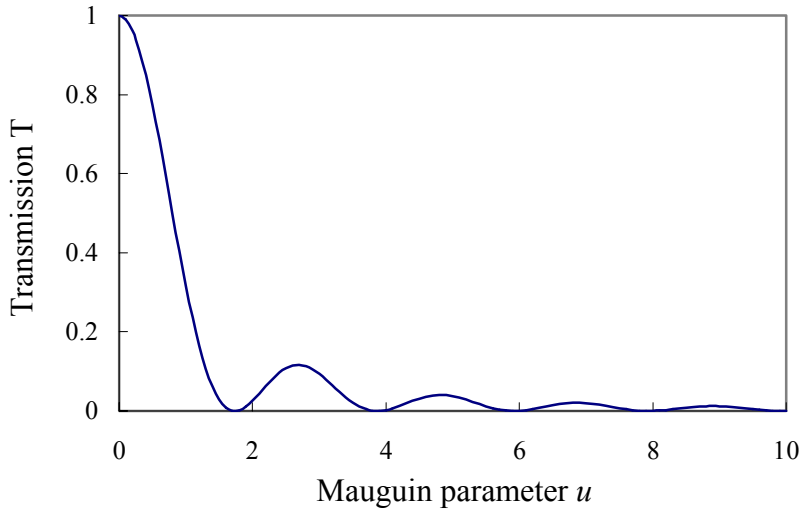

Fig. 4.12 The transmission T as a function of Mauguin parameter u

Consider a special case, it often happens in TNLC that the phase retardation Γ is much larger than the twist angle ϕ, the overall Jones matrix (*Eq*. (4.25)) becomes

$$M = R(\phi)\begin{pmatrix} e^{-i\Gamma/2} & 0 \\ 0 & e^{i\Gamma/2} \end{pmatrix} \tag{4.29}$$

For an incident light is linearly polarized along one of the principle axes, then according to matrix of *Eq*. (4.29), the light beam only "gains" a phase shift and leaves the polarization state unchanged. Thus if the incident light is polarized along the normal modes at the input plane, the polarization vector of the light will follow the rotation of the principle axes and remain parallel to the local slow (or fast) axis. This is called adiabatic following. In above case (ϕ=π/2), the polarization vector follows the rotation of axes and therefore is rotated by an angle of 90°. Since this direction is orthogonal to the transmission axis of the second polarizer, the transmission is zero (Fig. 4.13(a), LC off-state). It can be realized in Fig. 4.12 when u is large. Thus the 90° TNLC cell sandwiched between a pair of parallel polarizers is called normally black mode. On the contrary, if the TNLC cell is placed between two crossed polarizers, the incident ray will pass through the second polarizer. It is called normally white mode. If the TNLC cell is now under an external electric field, alignment of the molecules is subjected to competing effect of the field and the wall. For a sufficiently intense electric field all the molecules are aligned parallel to the electric field, which is perpendicular to the easy

direction i.e. perpendicular to the surfaces of the glass substrates except for those adjacent to the polyimide surfaces. The polarization of the light passing through the TNLC will not change. In normally black mode, the light will pass though the second polarizer when applying a sufficiently intense electric field (Fig. 4.13(b), LC on-state).

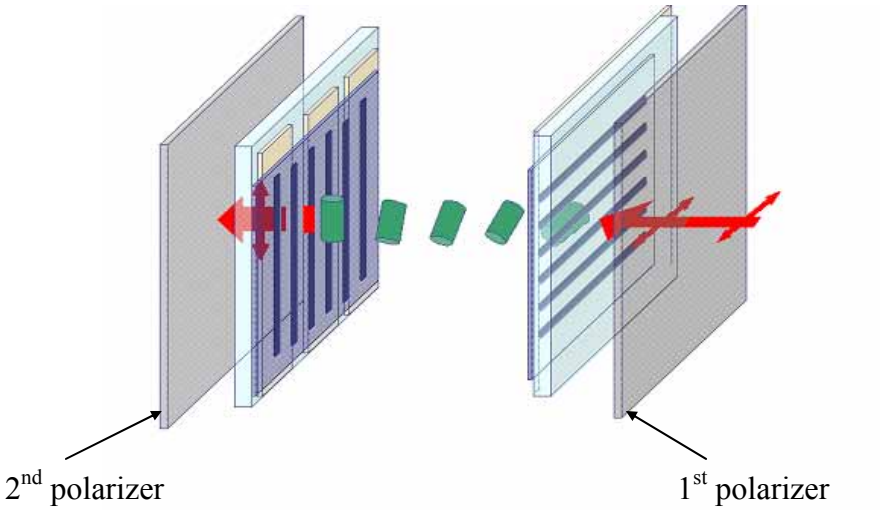

(a)

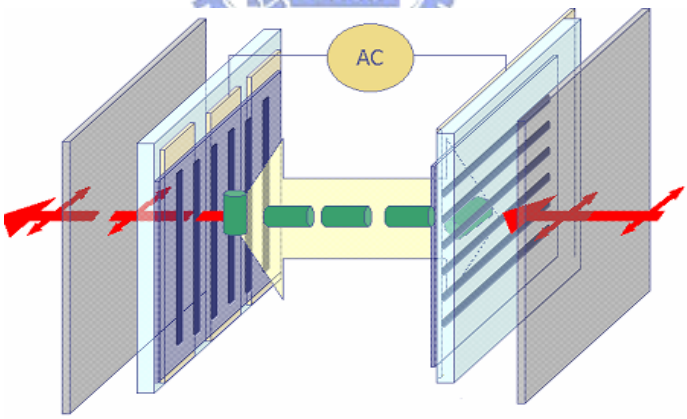

(b)

Fig. 4.13 TNLC cell of normally black mode in (a) off-state and (b) on-state

According to *Eq.* (4.28), we can design a normally black mode TNLC. For E7, $\Delta n = n_e - n_o = 0.198$ at $\lambda = 780$ nm. We plot transmission T as a function of TNLC thickness *d* in Fig.4.14.

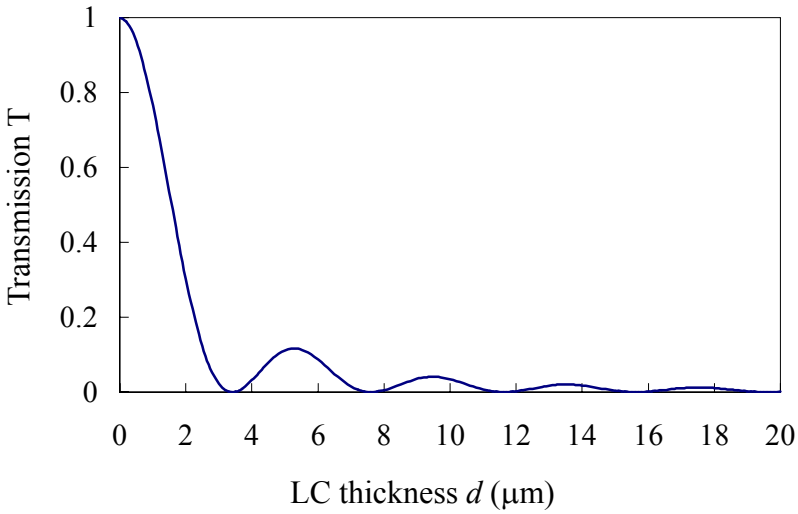

Fig. 4.14 The transmission T as a function of LC thickness *d*.

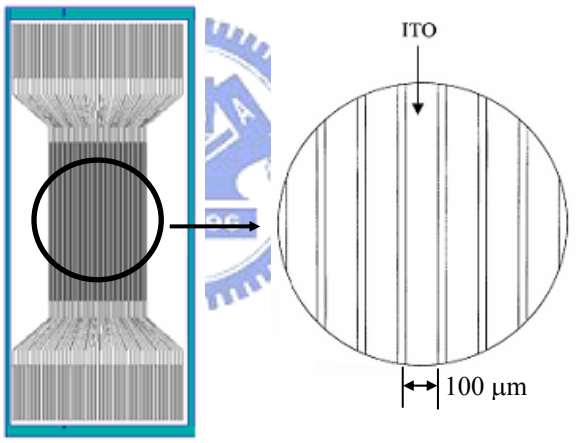

Fig. 4.15 The ITO pattern

We design the TNLC cell in the normally black mode. In our design, a 90° TNLC cell is constructed with a 6-μm-thick NLC (E7 manufactured by Merck) layer sandwiched between ITO glass plates. The patterned ITO electrodes as shown in Fig. 4.15 consist of fifty 100 μm × 2 cm stripes with 5-μm spacing. The TNLC cell is bonded to a polarizer with its direction is parallel to the polarization direction of the incident laser beam. An Au-coated silicon substrate is bonded to the polarizer as the back mirror. When the LC is in off state, light will not pass through the polarizer and thus no light is reflected. When the LC is under an external electric field, i.e. on state, the light will pass through and is reflected by the back mirror. The cell

thickness of 6-μm is designed for wavelength of 1.5 μm for other applications. According to our design (Fig. 4.14), the transmission T of 6-μm thickness is not zero but it is small enough in our applications.

4.4.2 LCPM based ECDL

A LCPM based ECDL is shown in Fig. 4.16. It is a folded telescopic grazing-incidence grating-loaded external cavity [63] incorporating a LCPM. An AR-coated LD is used as the gain medium. The output light of the LD is collimated by an objective, then incident on a diffraction grating. The first-order-diffracted light from the grating is collected by an imaging lens and focused on the LCPM. The zero-order reflection from the grating is the laser output.

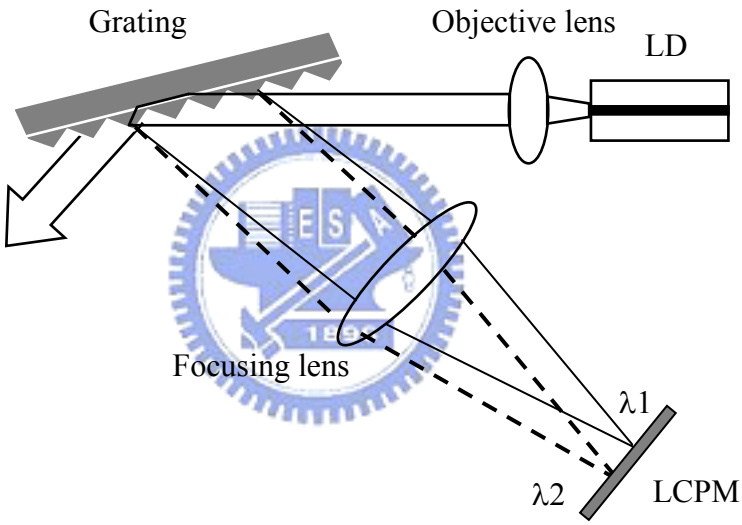

Fig. 4.16 LCPM based ECDL. LD: laser diode; LCPM: liquid crystal pixel mirror

The laser configuration is based on the spatial dispersion of the grating and the transmitted wavelength is selected by the LCPM. According to the grating equation (4.1), the differentiation is given as below

$$d\lambda = a\cos\theta_m d\theta_m \tag{4.30}$$

where a is the groove spacing of the grating , θ_m is the angle of the first-order diffraction, f_{lens} is the focal length of the imaging lens. At the focal plane, we obtained different displacement with changing the angle of the first-order diffraction

$$dx = f_{lens} \cdot a \tan \theta_m \approx f_{lens} \cdot a \theta_m \tag{4.31}$$

Narrow-band laser oscillation at the desired wavelength is realized by electronically selected optical feedback of the retro-reflected light from one pixel of the LCPM to the LD. Substituting $d\theta_m$ of *Eq.* (4.31) into *Eq.* (4.30), we can derive the relations of the wavelength variation $d\lambda$ and the lateral displacement dx as

$$d\lambda = \frac{a \cos \theta_m}{f_{lens}} dx \tag{4.32}$$

Assume a laser beam incidents on a 1800 lines/mm diffraction grating at an angle of 80°. The laser wavelength is 775 nm. The focal length of the imaging lens is 150 mm and the pixel pitch of the LCPM is 105 μm. According to *Eq.* (4.1) and (4.32), the relations of the wavelength variation and the lateral displacement are $d\lambda/dx$=3.378 nm/mm.